



# Assessment of trends, variability and impacts of droughts across Brazil over the period 1980–2019

Javier Tomasella<sup>1</sup> · Ana Paula M. A. Cunha<sup>1</sup> · Paloma Angelina Simões<sup>2</sup> · Marcelo Zeri<sup>1</sup>

Received: 16 June 2021 / Accepted: 5 December 2022 / Published online: 16 December 2022  
© The Author(s), under exclusive licence to Springer Nature B.V. 2022

## Abstract

Drought indices are a numerical representation of drought conditions aimed to provide quantitative assessments of the magnitude, spatial extent, timing, and duration of drought events. Since the adverse effects of droughts vary according to the characteristics of the event, the socioeconomic vulnerabilities, exposed communities or environments, there is a profusion of drought indicators to assess drought impacts in different sectors. In this study, we evaluated the performance of two drought indices, the Standardized Precipitation Index—SPI and Standardized Precipitation Evapotranspiration Index—SPEI over Brazil derived from gridded meteorological information over the period 1980–2019. Firstly, we compared the gridded derived indices against the same indices derived from weather station data and available from a global dataset for time scales of 3, 6, 12, 24 months. Then we analyzed the spatio-temporal trends in SPI and SPEI time-series, which revealed statistically significant trends toward drier conditions across central Brazil for all time scales, though with more intensity for time scales of 12 months and larger. Trends were more significant in magnitude for SPEI than SPI, indicating an important role in the increase in evaporation, driven by increasingly higher temperatures. Finally, we demonstrated that climate signals are already having a disruptive effect on the country's energy security.

**Keywords** Drought trends · SPI · SPEI · Impacts

## 1 Introduction

Drought is a natural climatic event which affects all ecosystems, either in arid lands or rainforests (Dai 2011; Svoboda and Fuchs 2017; Wang et al. 2017). As a hazard, drought is primarily defined as a period in which precipitation is less than the long-term average, resulting in a water shortage. In the disaster context, drought takes place over densely populated

---

✉ Javier Tomasella  
javier.tomasella@cemaden.gov.br

<sup>1</sup> Centro Nacional de Monitoramento e Alertas de Desastres Naturais, CEMADEN, Estrada Doutor Altino Bondensan, 500, São José dos Campos, SP 12247-016, Brazil

<sup>2</sup> Universidade Federal de Itajubá (UNIFEI), Av. B P S, 1303, Pinheirinho, Itajubá, MG 37500-903, Brazil

areas and/or over vulnerable environments, and can result in disaster when local capacities are insufficient to avoid significant damage or losses (Wilhite 2000; Cunha et al. 2019a).

During the last decade, Brazil has been castigated by widespread droughts which affected all country's regions (Rodrigues and McPhaden 2014; Coelho et al. 2016; Nobre et al. 2016; Jiménez-Muñoz et al. 2016; Erfanian et al. 2017; Marengo et al. 2017, 2018b, 2021; Tomasella et al. 2018; Brito et al. 2018; Cunha et al. 2019b; Ferreira da Silva et al. 2020; De Medeiros et al. 2021). This is particularly worrying, since droughts in Brazil are associated with severe economic and social impacts, affecting more people than any other natural disaster (EM-DAT 2021; S2ID 2021).

Several studies pointed out that climate change is likely to increase the frequency and magnitude of future droughts (Dai 2013; Marengo et al. 2017, 2018a; IPCC 2018; Vogel et al. 2020). In this context, a larger number of drought and heat waves events in Brazil poses a severe threat to agriculture production (Martins et al. 2019), hydropower generation (von Randow et al. 2019), drinking water supplies (Marengo et al. 2020), desertification (Vieira et al. 2021a, b) and social vulnerability (Vieira et al. 2020).

Identifying early warning signals of major droughts in the country's most critical hot-spots are crucial for an effective preparedness plan and drought mitigation and adaptation. Drought characterization is essential to enable drought early warning and for risk analysis and management. To this end, selecting drought indicators (or indices) to be used by decision-makers is considered one of the most crucial components of any early warning system.

Drought indices allow for the characterization, quantification, and communication of the phenomenon (Gupta et al. 2011). There are many indicators and indices for the drought hazard assessment based on various information sources (Svoboda and Fuchs 2017). The choice of indicators and indices depends on the data availability, the study region (the size of the area), the time scale (seasonal, annual, decadal, etc.), and the drought typology (agricultural, hydrological, ecological, etc.). The most common drought indicators are precipitation, temperature, soil moisture, vegetation condition, and reservoir levels (Svoboda and Fuchs 2017). Since drought is a climatological hazard (Hisdal and Tallaksen 2000; EM-DAT 2021), the basis of drought indices mostly depends on the deviations of indicators values from the long-term mean.

One of the most common drought indices is the Standardized Precipitation Index (SPI), developed by McKee et al., (1993) and recommended by the World Meteorological Organization (Svoboda and Fuchs 2017). SPI is based on the normalization of precipitation probabilities and can identify extreme climate events (dry or wet) at different time scales. A drought event is identified when SPI values become continuously negative and reach  $-1$ , which are considered rare based upon the region's climate being investigated. Despite being widely used and recommended by the WMO, one of the weaknesses of the SPI is that it does not consider the influence of other variables on drought conditions, which makes it not appropriate to identify warming-related drought impacts on different environments (Vicente-Serrano et al. 2013).

Most recently, Vicente-Serrano et al. (2010a, b) developed the Standardized Precipitation Evapotranspiration Index (SPEI), which considers the variability of both precipitation and potential evaporation to assess drought conditions in a region, recognizing that temperature is an important climatic factor that influences water availability (Tirivarombo et al. 2018). The SPEI is based on climatic water balance (precipitation minus evaporation) and can show a more realistic result than the SPI, in particular in those regions where the potential evaporation is higher than annual precipitation. In

those cases, a precipitation-only based drought index may not accurately represent the drought condition (Begueria et al. 2014; Tirivarambo et al. 2018).

Drought indices must be calculated from ground station datasets to achieve a more accurate analysis of drought conditions. However, the lack of a long enough and consistent time series are the major obstacle to the study and monitoring the spatial pattern of droughts. Despite this, drought indices have been calculated from data sets available at regional and global scales (Vicente-Serrano et al. 2015; Tirivarambo et al. 2018) since they represent a reasonably long-time series (> 30 years).

Several studies worldwide have compared the performance of the various available drought indices, besides SPI and SPEI, for detecting and quantifying the magnitude of droughts. Wang et al. (2017), for instance, compared SPI and SPEI for various sub-regions of Northwestern China and found a close agreement between both indices, though the highest correlations were found at 16–36 months. Differences with both indices were attributed to the relative importance of evaporation compared to precipitation. Another performance study conducted by Wable et al. (2019) in a semiarid river basin in India using several drought indices, in addition to SPI and SPEI, revealed that SPEI-09 has a better performance. A comparison of the performance of SPI and SPEI in the Yangtze River Basin (Li et al. 2019) indicated a superior performance of SPEI, particularly when evaporation is estimated using the Penman–Monteith method. In inner Mongolia, (Pei et al. 2020) revealed temporal consistency between SPI and SPEI, though differences appeared between the indices at short timescales. The authors concluded that SPEI may be more suitable than the SPI for drought monitoring.

Very few studies in Brazil use SPEI index as an indicator of drought. For instance, Rocha Júnior et al. (2019) used SPEI to investigate trends in the climatological wettest trimesters in the northeast of Brazil (NEB). Bevacqua et al. (2021) investigated hydrologic drought propagation based on the time-lag between drought onset, indicated by SPEI, and the hydrological impact in main basins in Brazil as indicated by a streamflow index. No previous studies have assessed the use of SPEI for the whole country from a hazard monitoring perspective.

Despite the fact that previous studies have suggested that SPEI could be more appropriate than precipitation-based indexes, operational drought early warning systems in Brazil do not use SPEI in combination with FAO56 Penman–Monteith method, which is a superior method to estimate potential evaporation. Therefore, considering the wide variety of climate regimes that characterized Brazil, the potential impact of using SPEI (in combination with a physically based mass transfer evaporation equation) for drought assessment is worthy to be investigated.

Because of the complex characteristics of the phenomena, there is a consensus that no particular index alone is suitable for characterizing all droughts typologies in all places and time-periods (Svoboda et al. 2015). In this context, it is critical to analyze the efficiency of drought indices, specifically those that combine simplicity with robustness such as SPI and SPEI. Therefore, the main goal of this study is to compare SPI and SPEI, both spatially and temporally, for the whole country using the most recent available datasets and station data. This is a necessary step for improving operational drought assessment products such as those available at the National Center for Monitoring and Early Warning of Natural Disasters (CEMADEN).

Finally, we investigated trends in SPI and SPEI series to determine if the recent droughts that affected Brazil indicate an increased frequency of extreme events, as suggested by climate change scenarios (Vogel et al. 2020), and which regions of the country have been affected more severely.

## 2 Data and methodology

### 2.1 Site description

Brazil has an area of 8.5 mi km<sup>2</sup> which includes diverse climate regimes, biomes, soils, and consequently water availability. The main biomes in Brazil are Amazon (49.3%), Cerrado (23.9%), Atlantic Forest (13%), Caatinga (9.9%), Pampa (2.1%) and Pantanal (1.8%) (Figueiredo 2016). According to (Alvares et al. 2013) the main Koppen's climate zones in Brazil are Tropical (81.4%), Humid Subtropical (13.7%) and Dry (4.9%) (Fig. 1).

Except for the southern region and part of the Amazon, in general, the annual rainfall regime in most of Brazil is well defined, with the rainy season starting in mid-October and ending in April and a dry season between May and September (Reboita et al. 2010). However, the spatial patterns of rainfall and temperature in Brazil are also quite irregular. The annual accumulated rainfall ranges from ~400 mm/year in the semiarid region to more than 2500 mm/year in the northwest region of the Amazon. The average annual temperature ranges from ~15 C in the South to ~28 C in the far north of the country (INMET 2021).

The large area of the country, added to social disparities and heterogeneous ecosystems, determine a wide variety of drought impacts.

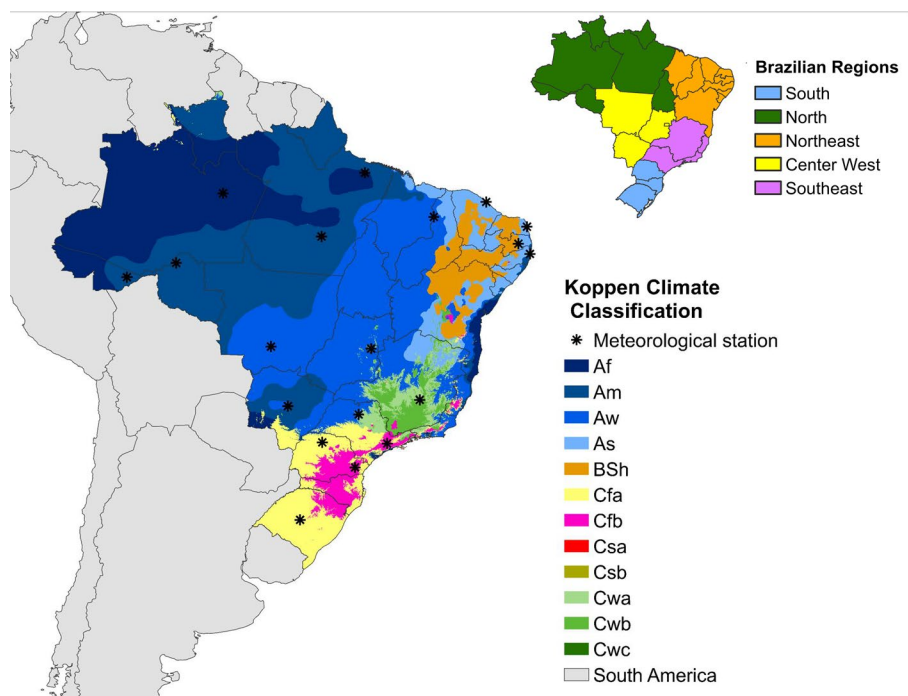


**Fig. 1** Geographical location of the study area, the main climate types according to Koppen classification (Alvares et al. 2013), and the location of meteorological stations used to calculate drought indices

## 2.2 In situ meteorological data

Table 1 shows the description of the 19 meteorological stations used to calculate the SPI and SPEI time-series. The data set consists of measured weather data including air temperature (°C), maximum air temperature (°C), minimum air temperature (°C), atmospheric pressure (hPa), wind speed ( $\text{m}^2 \text{s}^{-1}$ ), air humidity (%) and insolation (h) for the period 1980–2016. Monthly variables were provided by the Brazilian National Institute of Meteorology – INMET (<https://portal.inmet.gov.br/servicos/bdmep-dados-historicos>).

Monthly averages over the period 1980–2016 of temperature, dew point, wind speed, atmospheric pressure, and insolation were used to calculate reference evaporation (Eto) using the FAO-56 Penman–Monteith equation as described by (Allen et al. 1998). The resulting time-series dataset of paired values of monthly precipitation and reference evaporation was used to calculate the SPI and SPEI indexes.

## 2.3 Gridded meteorological data

Daily gridded meteorological data, with a spatial resolution of  $0.1 \times 0.1$  degrees, were extracted from the database developed by Xavier et al. (2016; 2022), which is based on the interpolated ground-based observations from 9,259 rain gauges and 735 meteorological stations. This database includes, besides daily precipitation, ETo estimations using the FAO 56 Penman–Monteith method (Allen et al. 1998). More details about this dataset

**Table 1** Meteorological station locations and annual precipitation and mean temperature (Source: (INMET 2021))

Station name	Latitude (degrees)	Longitude(degrees)	Elevation (m)	Annual precipitation (mm)	Annual evaporation (mm)
Belém	−1.43	−48.43	7.13	3084.0	1888.7
Belo Horizonte	−19.93	−43.95	915.47	1602.6	1452
Brasília	−15.78	−47.92	1161.42	1477.4	1263.2
Campina Grande	−7.22	−35.90	546.27	777.0	1343.7
Campo Grande	−20.44	−54.72	528.43	1455.3	1753.7
Catanduva	−21.12	−48.94	570.34	1316.0	1738.7
Cuiabá	−15.61	−56.10	157.70	1454.5	2332.8
Curitiba	−25.44	−49.23	923.50	1575.8	1205.5
Fortaleza	−3.81	−38.53	29.89	1668.9	1969.5
Manaus	−3.10	−60.01	48.86	2301.2	2308.1
Maringá	−23.40	−51.91	542	1642.9	1673.8
Natal	−5.83	−35.20	47.68	1721.4	1841.1
Porto Velho	−8.79	−63.84	86.12	1875.9	1689.4
Recife	−8.05	−34.95	11.30	2263.4	1785.2
Rio Branco	−9.95	−67.86	160.71	1997.6	1847.1
Santa Maria	−29.72	−53.72	103.10	1796.2	1635.9
São Félix Do Xingu	−6.63	−51.97	195.98	2041.2	1733.9
São Paulo	−23.49	−46.61	785.16	1616.0	1409.1
Teresina	−5.03	−42.80	75.73	1325.0	2330

and detailed information on the interpolation method can be found in Xavier et al. (2016, 2022). We used gridded precipitation (P) and ETo series to generate SPI and SPEI time-series maps of the period 1980–2019.

## 2.4 SPI and SPEI processing

SPI was estimated using the methodology described by Guttman (1999). Rainfall data was fitted to a gamma probability density function with two parameters, estimated using the maximum likelihood approach described by Thom et al. (1966). Since the gamma distribution is not defined for nil values, we included the probability of zero rainfall when needed.

SPEI was derived using the methodology described by Beguería et al. (2014), which recommends fitting log-logistic statistical distribution of the differences in Precipitation and ETo. The parameters of the log-logistic distribution were calculated using the L moments procedure as described by Vicente-Serrano et al. (2010a, b) and using the unbiased estimator of the Probability Weighted Moment—PWM as recommended by Beguería et al. (2014).

For the analysis of the indices time-series, we considered cumulative values of P and P-ETo for time scales of 3, 6, 12, and 24 months.

## 2.5 Global SPEI dataset

For comparisons with our estimations, monthly SPEI maps from the global SPEI gridded dataset developed by Beguería et al. (2010) were used. The SPEIbase v.2.7 dataset covers the period 1901–2020 and offers global coverage at a 0.5 degree spatial resolution. In this updated version, the evapotranspiration was calculated based on the CRU-TS4.05 dataset (Harris et al. 2014) and using the FAO-56 Penman–Monteith equation (Allen et al. 1998). The CRU-TS4.05 represents a gridded climate dataset from monthly observations at meteorological stations across the world's land areas. A detailed description of SPEIbase can be found in Beguería et al. (2010) and (Vicente-Serrano et al. 2010a). The dataset is provided at <https://spei.csic.es/database.html>.

## 2.6 Validation

The SPI and SPEI time-series derived from the gridded P and ETo data of Xavier et al. (2022) were validated against SPI and SPEI (for 3, 6, 12, and 24 months) calculated from meteorological station data for the period 1980–2016. Comparisons were performed by extracting SPI and SPEI values from  $0.1 \times 0.1$  degrees pixel gridded data where the correspondent meteorological station was located. The comparison between the station data against the gridded database of Xavier et al. (2022) is relevant to ensure that the interpolation method is not smoothing climate trends, which is essential for both the assessment of the magnitude of the drought and in the detection of trends.

In addition, the SPEI time-series based on Xavier et al. (2016) were compared on a pixel-to-pixel basis of the global database of Vicente-Serrano et al. (2010b) for the period 1980–2019. Because the gridded global data set of Beguería et al. (2010) has a resolution of  $0.5 \times 0.5$ , SPEI time-series based on Xavier et al. (2022) were firstly resampled to the same resolution by averaging neighboring  $0.1 \times 0.1$  pixels to a single  $0.5 \times 0.5$  pixel.

The differences among SPI and SPEI values from different data sources were compared using scatter plots, density plots, histograms, and the Pearson correlation coefficient.

Also, we analyzed the time-variation consistency of selected 0.1 degrees pixel SPEI from Xavier et al. (2022) by comparing it with the SPEI series of the station located at the pixel. Finally, we analyzed the spatial pattern of the root-mean-squared differences—RMSD for the gridded data of Xavier et al. (2022) and (Vicente-Serrano et al. 2010a).

## 2.7 Trend analysis

After the SPI and SPEI series were validated against different data sources, trend analysis was conducted using the Mann Kendall trend test (Kendall 1975) for a significant level of 0.05 to identify areas with statistical significance.

## 3 Results

### 3.1 Comparison of SPI and SPEI from gridded products and station data

Figure 2 compares SPEI calculated from  $0.1 \times 0.1$  gridded meteorological data of Xavier et al. (2022), indicated as Xavier SPEI, against the values derived from the station data of Table 1 denoted as Station SPEI, both in terms of Pearson correlation and the correspondent histograms, for different time-steps. In terms of the agreement between Xavier-derived SPEI and station SPEI, Fig. 2 indicates correlation coefficients are above 0.72, while the histograms resulting from Xavier database show a higher frequency of values around -1 and 1.

Figure 3 shows a pixel-to-pixel comparison of SPEI gridded data extracted from Xavier et al. (2022) against those values from the global database of Vicente-Serrano et al.

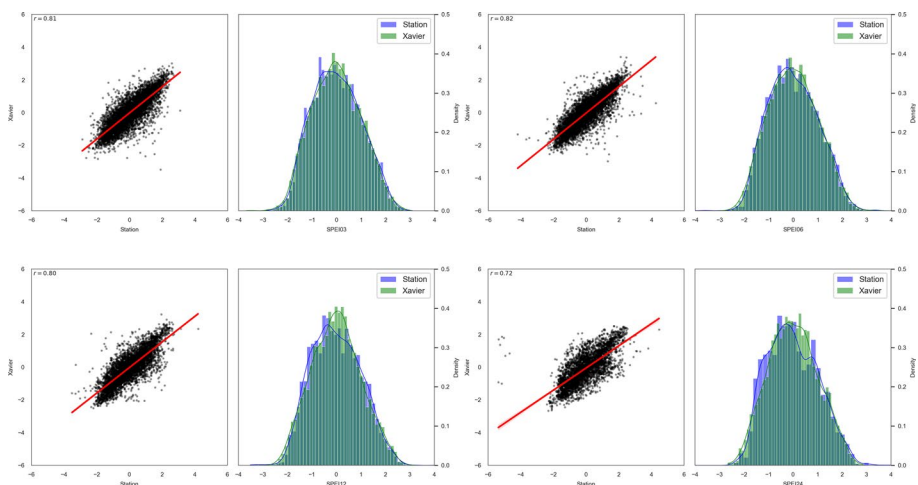


**Fig. 2** Scatter plots, density and histograms of SPEI values estimated using meteorological station data against the correspondent pixel SPEI derived from the gridded data of Xavier et al. (2016), for the period 1981–2016 and for different timescales



(2010b), for the period 1980–2019 and for different time-steps. As mentioned before, due to the spatial resolution of the global database, pixels correspond to 0.5 degrees. There is less agreement between both data sources in terms of the Pearson correlation compared with Fig. 2 for all timescales, and a decrease in correlation for larger time-steps. In terms of the density plots and histogram, and despite the coarser spatial resolution of the global data set, there is a close agreement between both datasets (Fig. 3). In general, SPEI from the Serrano database show lower frequencies close to neutral conditions ( $0.1 < \text{SPEI} < -0.1$ ) and higher frequencies for values at the extremes ( $-3 < \text{SPEI} < 3$ ).

We also analyzed the gridded products based on Xavier et al. (2016) and Vicente-Serrano et al. (2010b) in terms of spatial coherence. Figure S1 in supporting information shows the root-mean-squared differences (period 1980–2019) of the SPEI values of Xavier versus Serrano for various timescales. In general, differences are larger in Southern Amazonia, and along a strip in the southeastward direction of southeastern Brazil, and minimum for the rest of the eastern part of the country.

### 3.2 Trends analysis

Once the SPEI derived from the gridded data of Xavier et al. (2016) was validated with other sources of information, we analyzed trends of SPI and SPEI for the period 1980–2019. Figure 4 shows Kendall's tau values for the SPI and SPEI values derived from the gridded data of Xavier et al. (2022) for different timescales. Colored pixels indicate statistical significance for a confidence level below 0.05. The pixels in the red tone represent a significant SPEI decrease (drying trend), and the pixels in blue tones represent significant increasing trends of SPEI (more wet events).

Clearly, areas with statistical significance increase with the timescale, indicating that the magnitude of the trends becomes greater and widely spread for timescales of 12 and

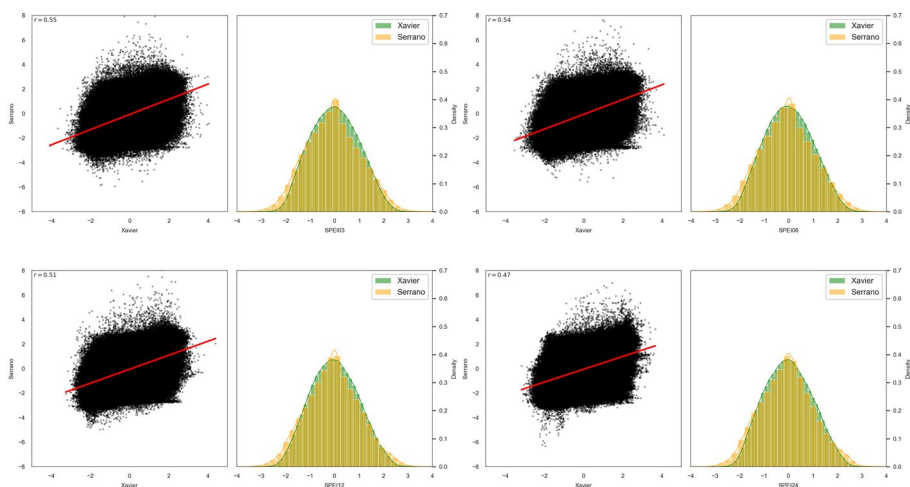


**Fig. 3** Scatter plots, density, and histograms comparing pixel-to-pixel SPEI values derived from the gridded data of Xavier et al. (2022) against Vicente-Serrano et al. (2010b), for the period 1980–2019 and for different timescales



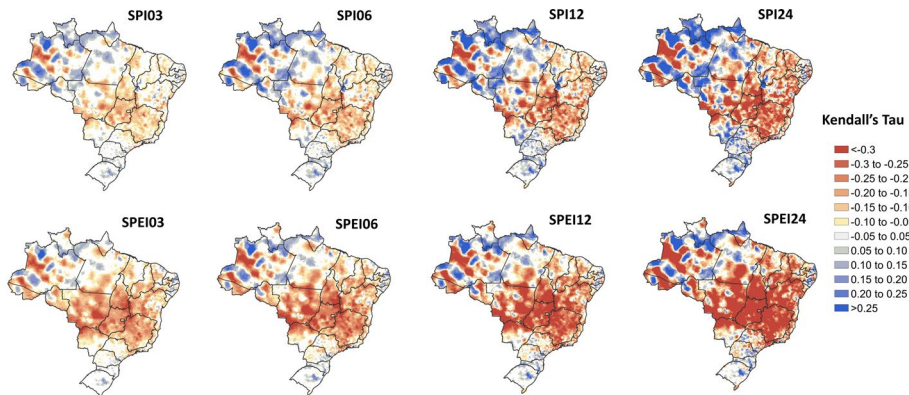


**Fig. 4** Kendall's tau values for SPI and SPEI values calculated from gridded data of Xavier et al. (2022) for the period 1980–2019 and for different timescales. Colored pixels indicate statistically significant values ( $p < 0.05$ )

24 months. Although trends also appear at the intraseasonal scale (3 to 6 months), they are less in magnitude and exhibit a more spatially spotty pattern.

Consistently negative trends, colored in red in Fig. 4, are recorded along the area of the influence of the South American Convection Zones—SACZ. The SACZ is a cloud band that extends from the intense convection region over the Amazon Basin south eastward into the South Atlantic Ocean (Seluchi and Marengo 2000) and transports moisture from the Amazon to Southeast Brazil. Intense rainfall events in Southeast and Central Brazil in the austral summer are closely linked to the position and persistence of the SACZ.

In agreement with previous results (Cunha et al. 2018; Carvalho 2020), negative trends are also evident in the Northeast of Brazil, where the principal mechanism producing rainfall is the meridional migration of the ITCZ (Hastenrath and Heller 1977). On the other hand, Northern Amazonia shows significant positive trends, which are consistent with the intensification of the hydrological cycle in northern Amazonia (Gloor et al. 2013). Positive trends were also detected in a region close to the coastal area of the Brazilian Northeast and South. More importantly, Fig. 4 clearly illustrates that the trends are much more significant and spatially homogeneous in the case SPEI compared to SPI. Consequently, it is clear that the magnitude of the trends are enhanced for the index that include reference evaporation.

In order to investigate why the trends observed in SPEI were much more significant when compared with those of SPI, the panel of Figure S2 in supplementary material shows Kendall's tau for monthly values of maximum (Tmax) and minimum temperature (Tmin), precipitation (P), and P-ET<sub>o</sub>. The top row maps indicate significant statistical positive trends toward increased Tmin and Tmax in most of Brazil, which is consistent with several previous studies (for instance, Salviano et al. 2016; Penereiro et al. 2018). On the other hand, the bottom row shows that significant trends for monthly precipitation are present only in a few areas in Brazil, mostly concentrated in the northern region. Besides, it shows a spatial distribution similar to SPI on the shorter time scale (Fig. 4). In contrast, the difference in P-ET<sub>o</sub> shows more significant decrease trends (dryness trends) than P, mainly in central Brazil. However, the significant areas are also smaller than those identified by SPEI on longer time scales (Fig. 4). Although the magnitude of trends in P-ET<sub>o</sub> is not more pronounced such as in the case of temperature, it is clear that those trends become more significant for increasing time-steps, as indicated by Fig. 4.

Based on this analysis, it is possible to conclude that there are statistically significant negative trends in both SPI and SPEI over the period 1980–2019 in most of Central Brazil, which becomes more significant for SPEI mostly related to the increase in evaporation associated with higher temperatures. Those trends become pronounced and spatially spread for larger timescales, indicating a gradual accumulation of deficits. This conclusion is further corroborated by Table 2, which shows the trend signals according to the Mann–Kendall test for P, SPI, SPIE, and Eto for the main political regions of Brazil (shown in Fig. 1). For rainfall, significant trends are detected for time steps greater than 12 months, negative for the Northeast, Central West, Southeast, and positive for the South and only for 12 months. In the case of reference evaporation, trends are significant and positive in the Central West and Southeast for all time-steps, for times steps greater than six months for the North and Northeast, and for all regions for time steps of 12 months and larger. Consequently, the influence of reference evaporation determines why trend signals are more significant for SPEI compared to SPI: Table 2 indicates that in the Central West and Southeast regions, significant negative signals are verified for SPI for time steps larger than 12 months, while these signals are detected for all time steps for SPEI.

### 3.3 Drought impacts

The area most affected by the negative trends of Fig. 4 includes regions heavily populated to the east, and almost the whole region of the country known as the new agricultural frontier in central Brazil within the Cerrado Biome, which is an area undergoing intense land use dynamics in recent decades and is responsible for the increase in grain production in Brazil (Vieira et al. 2021a, b).

**Table 2** Trend signals according to the Mann–Kendall test ( $p < 0.05$ ) for main Brazilian regions (depicted in Fig. 1) for Precipitation, SPI, SPIE, and Reference evaporation and for values accumulated for 3, 6 12, and 24 month time-steps

Index	Time Step (months)	North	Northeast	Central West	Southeast	South
Precipitation	03					
	06					
	12	+	–	–	–	+
	24	+	–	–	–	+
Reference Evaporation	03	+	+	+	+	
	06	+	+	+	+	
	12	+	+	+	+	+
	24	+	+	+	+	+
SPI	03			–	–	
	06	+	–	–	–	+
	12	+	–	–	–	+
	24	+	–	–	–	+
SPEI	03	–	–	–	–	
	06	–	–	–	–	
	12	–	–	–	–	
	24	–	–	–	–	

Land conversion from natural vegetation to pasture has been intensified in recent years along the agricultural frontier in the Cerrado biome (Beuchle et al. 2015). Zalles et al. (2019) reported that the cropland extent more than doubled in this biome across 2000 to 2014, while grain cultivation area increased by 80% between 1996 and 2006 (Merten and Minella 2013). Moreover, according to the Brazilian Atlas of Irrigation (ANA 2017), agricultural areas in central Brazil show the most intensive expansion of irrigation. Since irrigation and livestock production is the main consumptive use of Brazil, representing 80% of the country's total water use (Gesualdo et al. 2021), the uncontrolled expansion of irrigation is likely to trigger several water conflicts. Multsch et al. (2020) concluded that the expansion of irrigated area (45.6 Mha) predicted by the National Irrigation Policy (Law 12,787) is likely to drive 26.0 Mha under critical and very critical water scarcity in all the regions of Brazil, except Amazonia. Considering these calculations do not include the future climate change and the trends detected in this study, it is likely the estimations of Multsch et al. (2020) might be underestimating impacts.

In addition, the areas affected by negative trends in Fig. 4 correspond to the headwaters of the Paraná, Paraguay, São Francisco, and Tocantins rivers. Besides the importance of these basins for navigation and water supply, they host more than 90% of the country's hydropower installed capacity (ONS 2021). In this context, the blue line of Fig. 5 shows the stored energy in hydropower plants of the Center-West and Southeast interconnected subsystem of Brazil, which accounts for 70% of the total energy stored in hydropower plants for the period 2011–2020. According to the Brazilian Weather Forecast and Climate Studies Center—CPTEC (Rede Globo 2021), rainfall in both the Center-West and south-east of Brazil recorded values below average since 2011, which explain the decrease in stored energy in the country's most important subsystem. Because Brazil's economy has been facing slow economic growth and recession since 2012, which was amplified by the Covid-19 pandemic since 2020, it cannot be argued that the trend observed in Fig. 5 can be attributed to an increase in energy consumption.

Considering that 64% percent of Brazil's total electricity supply is provided by hydropower (ONS, 2021), climate oscillation affects hydroelectric outputs, and demand–supply

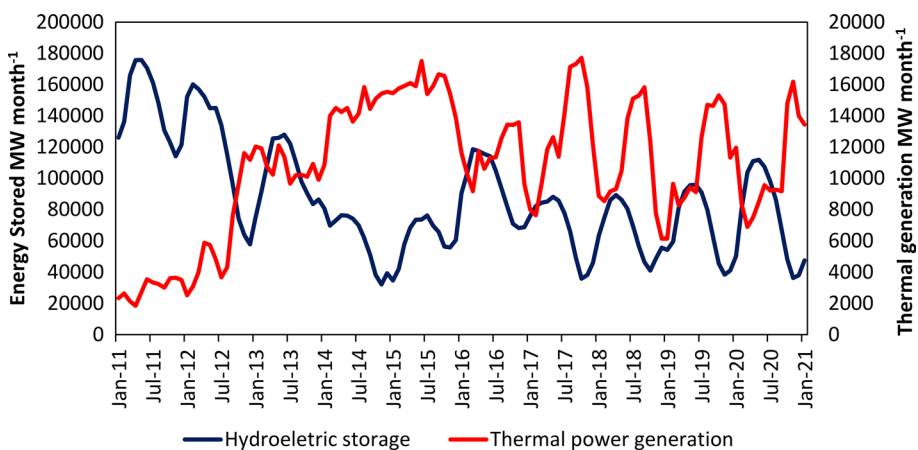


**Fig. 5** Stored energy in hydropower plants of the Center-West and Southwest of Brazil (blue line) and thermal power generation (red line) over the period 2011–2021 (Source: National System Operator—ONS Brazil)

needs to shift to higher-cost thermal power, a mixed of renewables and fossil fuel-based generation, during droughts. According to the Brazilian Association of Large Industrial Energy Consumers—ABRACE, energy prices increased 74% between 2011 and 2020 (Rede Globo 2021), related to the decrease in energy stored in hydropower plants concomitant with the increase in thermal generation (red line of Fig. 5).

Moreover, the possibility of increasing conflicts between irrigation and hydropower generation is no longer a likely scenario. An example of this is the Batalha hydropower plant in the Parana River headwater (Silva and Da Hora 2014), where the uncontrolled expansion of irrigation resulted in losses ranging from 8 to 19% in hydropower outputs.

Finally, the persistence of these trends might also have the potential to impact human consumption in the largest metropolitan areas of Brazil. A recent example is the precipitation deficits during 2014 and 2015, coupled with record temperatures that affected Southeast Brazil, which caused the “water crisis” in the São Paulo Metropolitan Area (Nobre et al. 2016). This situation demanded the implementation of drastic measures such as suspending the use of irrigation water in the basin and reducing pressure in the drinking water distribution network, which resulted in people being deprived of water for several hours a day, and in some cases, for several days. Trends toward increasing frequency of dry spells in the Metropolitan area of São Paulo (Marengo et al. 2020) suggest that the rainfall deficits observed during the water crisis of 2014 and 2015 are likely to become more frequent in future.

## 4 Discussion

SPEI and SPEI derived from gridded data from Xavier et al. (2022) showed close agreement to the correspondent indexes obtained from the station data, both in terms of the coefficient of determination and in the empirical distribution of the histograms. Differences between both datasets can be explained for several sources of uncertainties, such as interpolation of meteorological data, the effect of spatial resolution, and the data gaps of the station data, which might impact the fitted statistical distribution, particularly at the tails of the distribution.

As expected, comparison between SPI and SPEI between Xavier et al. (2022) and Vicente-Serrano et al. (2010b) on a  $0.5 \times 0.5$  degrees pixels basis revealed less agreement than in the case of the station data. Interpolated meteorological data from Xavier et al. (2022) uses the INMET meteorological stations (including those from Table 1), while the global database of Vicente-Serrano et al. (2010b) is derived from the CRU TS dataset, which is affected by larger uncertainties in regions with sparse data coverage (Harris et al. 2020), besides its coarser spatial resolution. In addition, the global database includes data for the period 1950–2020, which is used to fit the statistical distribution and might have affected the tail of the distribution.

Spatial analysis of the discrepancies is likely to be a combination of the poorer spatial coverage of station data in Serrano’s products, especially in the Amazonia and the Center-West region as also indicated by the cross-validation results of Harris et al. (2020). Because the density of stations in Brazil is lower mainly in the North and Center-West regions when compared to the rest of the country, a small number of additional weather stations included in Xavier’s database in areas with poor data coverage have a significant impact in the interpolation. Nevertheless, agreement between both datasets is remarkable taken into account differences in data sources, data processing and the period of analysis.

SPI and SPEI trend analysis indicates positive trends in the extreme north and south of Brazil and negative trends in the rest of the country. Regarding the physical mechanisms involved in the observed trends, there is no consensus whether these modifications in the climate regime are caused by changes in decadal variability and/or the global warming trend, either on a regional or global scale (Geng et al. 2019). Although those trends can be related to variations at interdecadal timescales related to teleconnection patterns (Grimm and Saboia 2015; Espinoza et al. 2019; Prado et al. 2021), trends in the last decades have also been associated to global warming (Penereiro et al. 2018) and regional land use and land cover changes (de Oliveira et al. 2021). Combination of these effects might produce results that appeared to be contradictory. For instance, a recent study by Marengo et al. (2020) concluded that the São Paulo Metropolitan Area showed a positive trend in annual precipitation mainly due to an increase in the frequency of extreme precipitation events, concomitant with a decrease in the number of consecutive dry days. This result indicates that intense precipitation is concentrated in fewer days separated by longer dry spells, which can be partly explained by natural climate variability, global warming and/or urbanization (Marengo et al. 2020) and provides an additional explanation for the results shown in Fig. 4.

Finally, it is worth mentioning that the projections of the Sixth Assessment Report of the Intergovernmental Panel on Climate Change (IPCC, 2021) show the same spatial patterns observed in Fig. 4, i.e., wetter conditions in the south of Brazil and drier conditions in the rest of the country. IPCC scenarios indicate the same pattern even in the case of the milder climate change scenario (Paris agreement), though changes are exacerbated under higher warming.

## 5 Conclusions

During the period 2011–2019, droughts affected all Brazil's regions, resulting in profound ecological, social, and economic impacts. Although most of Brazil is a country rich in water availability, droughts are ecologically disruptive due to water scarcity and because they were associated with the occurrence of major fires and soil degradation. Additionally, it affected the population and caused heavy economic losses in agriculture, power generation, water supply, navigation, and irrigation.

Considering that previous studies have suggested that SPEI could be more appropriate than precipitation-based indexes to monitor drought conditions potentialized by warming conditions, in this study we evaluated the use of SPEI as a drought indicator calculated from a global dataset (SPEI-Serrano) and a regional dataset (SPEI-Xavier). The results showed that SPEI-Xavier is consistent with observed data, and its useful to monitor drought conditions or assess changes in drought patterns should be encouraged.

Previous studies of trends were mainly based on rainfall series and/or temperature at monthly timescales, which generally produced inconclusive results, particularly for rainfall. The use of SPI and SPEI-Xavier for drought assessment revealed significant drought trends at all timescales, but higher in magnitude and spatial extent for timescales longer than 12 months, indicating cumulative effects of water deficits. Moreover, trends toward drier conditions detected in the central areas of Brazil were exacerbated by the SPEI index, indicating a conjoint effect of rainfall and evaporation, mostly associated with the increase in temperature.

Although we cannot discriminate how much of the detected trends can be attributed to decadal variability and global warming trends, it is important to emphasize that those trends are consistent with global warming scenarios. The persistence of those signals implies an additional challenge for water resources and ecological management and the need to rethink public policies. Hydropower generation has already been affected, and water shortages such as those experienced recently in urban areas are likely to repeat in the near future. Several adaptation measurements will be necessary under such scenarios, such as those already implemented in the metropolitan area of São Paulo in the aftermath of the 2014 water crisis.

In addition, it is clear that irrigation policies need to be revisited, and the adoption of more efficient irrigation systems is needed. Because Brazil became a big player in agricultural commodities exports to the global market in the last two decades, efficient and integrated water resources management of water use to achieve sustainability is undoubtedly the most serious challenge to be faced by the country in the next decade.

**Supplementary Information** The online version contains supplementary material available at <https://doi.org/10.1007/s11069-022-05759-0>.

**Acknowledgements** This work was partially supported by the Brazilian National Council for Scientific and Technological Development (CNPq)

**Author contributions** JT and APC Conceptualization, Methodology, Software, Formal analysis, Visualization, Writing; PAS Data collection and Analysis; MZ Data collection and Analysis.

**Funding** Conselho Nacional de Desenvolvimento Científico e Tecnológico – CNPq/Brazil.

**Availability of data and material** All data should be made available on request to the authors.

**Code availability** Not applicable.

## Declarations

**Conflict of interest** The authors declare that they have no known competing financial interests or personal.

**Ethics approval** Not applicable.

**Consent to participate** Not applicable.

**Consent for publication** Not applicable.

## References

- Allen RG, Pereira LS, Raes D, Smith M (1998) Crop evapotranspiration: guidelines for computing crop requirements. *Irrig Drain*. <https://doi.org/10.1016/j.eja.2010.12.001>
- Alvares CA, Stape JL, Sentelhas PC et al (2013) Köppen's climate classification map for Brazil. *Meteorol Zeitschrift* 22:711–728. <https://doi.org/10.1127/0941-2948/2013/0507>
- ANA (2017) Atlas Irrigação - Uso da água na agricultura irrigada. [https://biblioteca.ana.gov.br/asp/download.asp?codigo=148256&tipo\\_midia=2&iIndexSrv=1&iUsuario=0&obra=88090&tipo=1&iBanner=0&iIdioma=0](https://biblioteca.ana.gov.br/asp/download.asp?codigo=148256&tipo_midia=2&iIndexSrv=1&iUsuario=0&obra=88090&tipo=1&iBanner=0&iIdioma=0)
- Beguieria S, Vicente-Serrano SM, Angulo-Martínez M (2010) A multiscalar global drought dataset: the SPEI base: a new gridded product for the analysis of drought variability and impacts. *Bull Am Meteorol Soc* 91:1351–1354. <https://doi.org/10.1175/2010BAMS2988.1>

- Beguieria S, Vicente-Serrano SM, Reig F, Latorre B (2014) Standardized precipitation evapotranspiration index (SPEI) revisited: parameter fitting, evapotranspiration models, tools, datasets and drought monitoring. *Int J Climatol* 34:3001–3023. <https://doi.org/10.1002/joc.3887>
- Beuchle R, Grecchi RC, Shimabukuro YE et al (2015) Land cover changes in the Brazilian Cerrado and Caatinga biomes from 1990 to 2010 based on a systematic remote sensing sampling approach. *Appl Geogr* 58:116–127. <https://doi.org/10.1016/j.apgeog.2015.01.017>
- Bevacqua A, Chaffe P, Chagas V, Agha KA (2021) Spatial and temporal patterns of propagation from meteorological to hydrological droughts in Brazil. *J Hydrol* 603:126902. <https://doi.org/10.1016/j.jhydrol.2021.126902>
- Brito SSB, Cunha APMA, Cunningham CC et al (2018) Frequency, duration and severity of drought in the semiarid Northeast Brazil region. *Int J Climatol* 38:517–529. <https://doi.org/10.1002/joc.5225>
- Carvalho LMV (2020) Assessing precipitation trends in the Americas with historical data: a review. *Wiley Interdiscip Rev Clim Chang* 11:e627. <https://doi.org/10.1002/wcc.627>
- Coelho CAS, de Oliveira CP, Ambrizzi T et al (2016) The 2014 southeast Brazil austral summer drought: regional scale mechanisms and teleconnections. *Clim Dyn* 46:3737–3752. <https://doi.org/10.1007/s00382-015-2800-1>
- do Amaral Cunha AP, Marchezini V, Lindoso DP, Saito SM, dos Santos Alvalá RC (2019) The challenges of consolidation of a drought-related disaster risk warning system to Brazil. *Sustentabilidade em Debate* 10(1): 43–76
- Cunha APMA, Tomasella J, Ribeiro-Neto GG et al (2018) Changes in the spatial–temporal patterns of droughts in the Brazilian Northeast. *Atmos Sci Lett* 19:e855. <https://doi.org/10.1002/asl.855>
- Cunha APMA, Zeri M, Deusará Leal K et al (2019) Extreme drought events over Brazil from 2011 to 2019. *Atmosphere* 10:642. <https://doi.org/10.3390/atmos10110642>
- Dai A (2011) Drought under global warming: a review. *Wiley Interdiscip Rev Clim Chang* 2:45–65. <https://doi.org/10.1002/wcc.81>
- Dai A (2013) Increasing drought under global warming in observations and models. *Nat Clim Chang* 3:52–58. <https://doi.org/10.1038/nclimate1633>
- De Medeiros FJ, De Oliveira CP, Gomes RDS et al (2021) Hydrometeorological conditions in the semiarid and east coast regions of northeast Brazil in the 2012–2017 period. *An Acad Bras Cienc* 93:1–15. <https://doi.org/10.1590/0001-3765202120200198>
- de Oliveira RG, Valle Júnior LCG, da Silva JB et al (2021) Temporal trend changes in reference evapotranspiration contrasting different land uses in southern Amazon basin. *Agric Water Manag* 250:106815. <https://doi.org/10.1016/j.agwat.2021.106815>
- EM-DAT (2021) The International Disaster Databse. <https://www.emdat.be/>. Accessed 20 Jan 2001
- Erfanian A, Wang G, Fomenko L (2017) Unprecedented drought over tropical South America in 2016: Significantly under-predicted by tropical SST. *Sci Rep* 7:5811. <https://doi.org/10.1038/s41598-017-05373-2>
- Espinoza JC, Ronchail J, Marengo JA, Segura H (2019) Contrasting North–South changes in Amazon wet-day and dry-day frequency and related atmospheric features (1981–2017). *Clim Dyn* 52:5413–5430. <https://doi.org/10.1007/s00382-018-4462-2>
- Ferreira da Silva GJ, de Oliveira NM, Santos CAG, da Silva RM (2020) Spatiotemporal variability of vegetation due to drought dynamics (2012–2017): a case study of the Upper Paraíba River basin, Brazil. *Nat Hazards* 102:939–964. <https://doi.org/10.1007/s11069-020-03940-x>
- Figueiredo AH de (2016) Formação territorial. In: *Brasil : uma visão geográfica e ambiental no início do século XXI*
- Geng T, Yang Y, Wu L (2019) On the mechanisms of Pacific decadal oscillation modulation in a warming climate. *J Clim* 32:1443–1459. <https://doi.org/10.1175/JCLI-D-18-0337.1>
- Gesualdo G, Sone JS, de Galvão O C et al (2021) Unveiling water security in Brazil: current challenges and future perspectives. *Hydrol Sci J* 66:759–768. <https://doi.org/10.1080/02626667.2021.1899182>
- Gloor M, Brienens RJW, Galbraith D et al (2013) Intensification of the Amazon hydrological cycle over the last two decades. *Geophys Res Lett* 40:1729–1733. <https://doi.org/10.1002/grl.50377>
- Grimm AM, Saboia JPI (2015) Interdecadal variability of the south American precipitation in the monsoon season. *J Clim* 28:755–775. <https://doi.org/10.1175/JCLI-D-14-00046.1>
- Gupta AK, Tyagi P, Sehgal VK (2011) Drought disaster challenges and mitigation in India: Strategic appraisal. *Curr Sci* 100:1795–1806
- Guttman NB (1999) Accepting the standardized precipitation index: a calculation algorithm. *J Am Water Resour Assoc* 35:311–322. <https://doi.org/10.1111/j.1752-1688.1999.tb03592.x>
- Harris I, Jones PD, Osborn TJ, Lister DH (2014) Updated high-resolution grids of monthly climatic observations - the CRU TS3.10 Dataset. *Int J Climatol* 34:623–642. <https://doi.org/10.1002/joc.3711>



- Harris I, Osborn TJ, Jones P et al (2020) Version 4 of the CRU TS monthly high-resolution gridded multi-variate climate dataset. *Sci Data* 7:109. <https://doi.org/10.1038/s41597-020-0453-3>
- Hastenrath S, Heller L (1977) Dynamics of climatic hazards in northeast Brazil. *Q J R Meteorol Soc* 103:77–92. <https://doi.org/10.1002/qj.49710343505>
- Hisdal H, Tallaksen LM (2000) Drought event definition. Assessment of the regional impact of droughts in Europe. Drought Event Definition. Technical Report 6.
- INMET (2021) Instituto Nacional de Meteorologia: Normais Climatológicas. <https://portal.inmet.gov.br/>. Accessed 20 Jan 2021
- IPCC (2018) Global warming of 1.5°C. <https://www.ipcc.ch/sr15/>. Accessed 16 June 2021
- IPCC (2021). Summary for Policymakers. In: Climate Change (2021) The Physical Science Basis. Contribution of Working Group I to the Sixth Assessment Report of the Intergovernmental Panel on Climate Change [Masson-Delmotte, V., P. Zhai, A. Pirani, S.L. Connors, C. Péan, S. Berger, N. Caud, Y. Chen, L. Goldfarb, M.I. Gomis, M. Huang, K. Leitzell, E. Lonnoy, J.B.R. Matthews, T.K. Maycock, T. Waterfield, O. Yelekçi, R. Yu, and B. Zhou (eds.)]. Cambridge University Press, Cambridge, United Kingdom and New York, NY, USA, pp. 3–32, doi:<https://doi.org/10.1017/9781009157896.001>.
- Jiménez-Muñoz JC, Mattar C, Barichivich J et al (2016) Record-breaking warming and extreme drought in the Amazon rainforest during the course of El Niño 2015–2016. *Sci Rep* 6:33130. <https://doi.org/10.1038/srep33130>
- Kendall MG (1975) Rank correlation methods. Griffin, London
- Li X, Sha J, Wang ZL (2019) Comparison of drought indices in the analysis of spatial and temporal changes of climatic drought events in a basin. *Environ Sci Pollut Res* 26:10695–11070. <https://doi.org/10.1007/s11356-019-04529-z>
- Marengo JA, Ambrizzi T, Alves LM et al (2020) Changing trends in rainfall extremes in the metropolitan area of são paulo: causes and impacts. *Front Clim* 2:3. <https://doi.org/10.3389/fclim.2020.00003>
- Marengo JA, Cunha AP, Cuartas LA et al (2021) Extreme drought in the Brazilian pantanal in 2019–2020: characterization, causes, and impacts. *Front Water* 3:13. <https://doi.org/10.3389/frwa.2021.639204>
- Marengo JA, Cunha AP, Soares WR, et al (2018a) Increase risk of drought in the semiarid lands of northeast Brazil due to regional warming above 4 °C. In: Climate Change Risks in Brazil. Ed Carlos A Nobre, Jose A Marengo, Wagner R Soares, Ana Paula Soares. Springer International Publishing
- Marengo JA, Torres RR, Alves LM (2017) Drought in Northeast Brazil—past, present, and future. *Theor Appl Climatol* 129:1189–1200. <https://doi.org/10.1007/s00704-016-1840-8>
- Marengo JAO, Alves LM, Alvala RCS et al (2018b) Climatic characteristics of the 2010–2016 drought in the semiarid northeast Brazil region. *An Acad Bras Cienc* 90:1973–1985. <https://doi.org/10.1590/0001-3765201720170206>
- Martins MA, Tomasella J, Dias CG (2019) Maize yield under a changing climate in the Brazilian Northeast: Impacts and adaptation. *Agric Water Manag* 216:339–350. <https://doi.org/10.1016/j.agwat.2019.02.011>
- McKee TB, Nolan J, Kleist J (1993) The relationship of drought frequency and duration to time scales. Prepr Eighth Conf Appl Climatol Amer Meteor, Soc
- Merten GH, Minella JPG (2013) The expansion of Brazilian agriculture: soil erosion scenarios. *Int Soil Water Conserv Res* 1:37–48. [https://doi.org/10.1016/S2095-6339\(15\)30029-0](https://doi.org/10.1016/S2095-6339(15)30029-0)
- Multsch S, Krol MS, Pahlow M et al (2020) Assessment of potential implications of agricultural irrigation policy on surface water scarcity in Brazil. *Hydrol Earth Syst Sci* 24:307–324. <https://doi.org/10.5194/hess-24-307-2020>
- Ning L, Liu J, Wang B et al (2018) Variability and mechanisms of megadroughts over eastern China during the last millennium: a model study. *Atmosphere* 10:7. <https://doi.org/10.3390/atmos10010007>
- Nobre CA, Marengo JA, Seluchi ME et al (2016) Some characteristics and impacts of the drought and water crisis in Southeastern Brazil during 2014 and 2015. *J Water Resour Prot* 8:252–262. <https://doi.org/10.4236/jwarp.2016.8.2022>
- ONS (2021) National System Operator Brazil. 2021. O sistema em números. <http://www.ons.org.br/paginas/sobre-o-sin/o-sistema-em-numeros>. Accessed 2 Mar 2021
- Pei Z, Fang S, Wang L, Yang W (2020) Comparative analysis of drought indicated by the SPI and SPEI at various timescales in inner Mongolia. *China Water* 12:1925. <https://doi.org/10.3390/w12071925>
- Penereiro JC, Badinger A, Maccheri NA, Meschiatti MC (2018) Distribuições de Tendências Sazonais de Temperatura Média e Precipitação nos Biomas Brasileiros. *Rev Bras Meteorol* 33:97–113. <https://doi.org/10.1590/0102-7786331012>
- Prado LF, Wainer I, Yokoyama E et al (2021) Changes in summer precipitation variability in central Brazil over the past eight decades. *Int J Climatol* 41:4171–4186. <https://doi.org/10.1002/joc.7065>

- Reboita MS, Gan MA, da Rocha RP, Ambrizzi T (2010) Regimes de precipitação na América do Sul: uma revisão bibliográfica. *Rev Bras Meteorol* 25:185–204. <https://doi.org/10.1590/s0102-77862010000200004>
- Rede Globo (2021) Energia mais cara: Centro-Oeste e Sudeste têm chuva abaixo da média em toda a última década. <https://g1.globo.com/economia/noticia/2021/02/13/energia-mais-cara-centro-oeste-e-sudeste-tem-chuva-abaixo-da-media-em-toda-a-ultima-decada.ghtml> Accessed 16/03/2021
- Rocha Júnior, R.L.; dos Santos Silva, F.D.; Lisboa Costa, R.; Barros Gomes, H.; Herdies, D.L.; Rodrigues da Silva, V.d.P.; Candido Xavier, A. Analysis of the Space–Temporal Trends of Wet Conditions in the Different Rainy Seasons of Brazilian Northeast by Quantile Regression and Bootstrap Test. *Geosciences* 2019, 9, 457. <https://doi.org/10.3390/geosciences9110457>
- Rodrigues RR, McPhaden MJ (2014) Why did the 2011–2012 la Niña cause a severe drought in the Brazilian Northeast? *Geophys Res Lett* 41:1012–1018. <https://doi.org/10.1002/2013GL058703>
- S. G, Chipanshi A., D S, A H (2014) Comparison of the SPI and SPEI on Predicting Drought Conditions and. In: Proceedings of the 28th Conference of Hydrology - 94th American Meteorological Society Annual Meeting. Atlanta (GA, USA), February 2–6. American Meteorological Society, Boston, MA, USA
- S2ID (2021) Sistema Integrado de Informações sobre Desastres. Available online: <http://www.mi.gov.br>. Accessed on 18 January 2021.
- Salviano MF, Groppo JD, Pellegrino GQ (2016) Distribuições de Tendências Sazonais de Temperatura Média e Precipitação nos Biomas Brasileiros. *Rev Bras Meteorol* 33:97–113. <https://doi.org/10.1590/0102-7786331012>
- Seluchi ME, Marengo JA (2000) Tropical–midlatitude exchange of air masses during summer and winter in South America: climatic aspects and examples of intense events. *Int J Climatol* 20:1167–1190. [https://doi.org/10.1002/1097-0088\(200008\)20:10%3c1167::aid-joc526%3e3.3.co;2-k](https://doi.org/10.1002/1097-0088(200008)20:10%3c1167::aid-joc526%3e3.3.co;2-k)
- Silva LMDC, Da Hora MDAGM (2014) Conflito pelo uso da água na Bacia Hidrográfica do Rio São Marcos: O estudo de caso da UHE Batalha. *Engevista* 17:166–174
- Svoboda M, Fuchs B (2017) Handbook of Drought Indicators and Indices. WMO. Geneva.
- Svoboda MD, Fuchs BA, Poulsen CC, Nothwehr JR (2015) The drought risk atlas: enhancing decision support for drought risk management in the United States. *J Hydrol* 526:274–286. <https://doi.org/10.1016/j.jhydrol.2015.01.006>
- Thom HCS, Organization WM, Climatology WG, on SM in, (1966) Some methods of climatological analysis. Secretariat of the World Meteorological Organization, Geneva
- Tirivarombo S, Osupile D, Eliasson P (2018) Drought monitoring and analysis: Standardised Precipitation Evapotranspiration Index (SPEI) and Standardised Precipitation Index (SPI). *Phys Chem Earth* 106:1–10. <https://doi.org/10.1016/j.pce.2018.07.001>
- Tomasella J, Silva Pinto Vieira RM, Barbosa AA et al (2018) Desertification trends in the Northeast of Brazil over the period 2000–2016. *Int J Appl Earth Obs Geoinf* 73:197–206. <https://doi.org/10.1016/j.jag.2018.06.012>
- Vicente-Serrano SM, Beguería S, López-Moreno JJ et al (2010a) A new global 0.5° gridded dataset (1901–2006) of a multiscale drought index: comparison with current drought index datasets based on the palmer drought severity index. *J Hydrometeorol* 11:1033–1043. <https://doi.org/10.1175/2010JHM1224.1>
- Vicente-Serrano SM, Beguería S, López-Moreno JJ (2010b) A multiscale drought index sensitive to global warming: the standardized precipitation evapotranspiration index. *J Clim* 23:1696–1718. <https://doi.org/10.1175/2009JCLI2909.1>
- Vicente-Serrano SM, Gouveia C, Camarero JJ et al (2013) Response of vegetation to drought time-scales across global land biomes. *Proc Natl Acad Sci U S A* 110:52–57. <https://doi.org/10.1073/pnas.1207068110>
- Vicente-Serrano SM, Van der Schrier G, Beguería S et al (2015) Contribution of precipitation and reference evapotranspiration to drought indices under different climates. *J Hydrol* 526:42–54. <https://doi.org/10.1016/j.jhydrol.2014.11.025>
- da Vieira RM, SP, Sestini MF, Tomasella J, et al (2020) Characterizing spatio-temporal patterns of social vulnerability to droughts, degradation and desertification in the Brazilian northeast. *Environ Sustain Indic* 5:100016. <https://doi.org/10.1016/j.indic.2019.100016>
- Vieira RMDSP, Tomasella J, Barbosa AA et al (2021a) Desertification risk assessment in Northeast Brazil: current trends and future scenarios. *L Degrad Dev* 32:224–240. <https://doi.org/10.1002/ldr.3681>
- Vieira RMDSP, Tomasella J, Barbosa AA, Polizel SP, Ometto JPHB, Santos FC, da Cruz Ferreira Y, de Toledo PM (2021b) Land degradation mapping in the MATOPIBA region (Brazil) using remote sensing data and decision-tree analysis. *Sci Total Environ* 782:146900. <https://doi.org/10.1016/j.scitotenv.2021.146900>

- Vogel MM, Hauser M, Seneviratne SI (2020) Projected changes in hot, dry and wet extreme events' clusters in CMIP6 multi-model ensemble. *Environ Res Lett* 15:094021. <https://doi.org/10.1088/1748-9326/ab90a7>
- Von Randow RCS, Rodriguez DA, Tomasella J et al (2019) Response of the river discharge in the Tocantins River Basin, Brazil, to environmental changes and the associated effects on the energy potential. *Reg Environ Chang* 19:93–204. <https://doi.org/10.1007/s10113-018-1396-5>
- Wable PS, Jha MK, Shekhar A (2019) Comparison of drought indices in a semi-Arid River basin of India. *Water Resour Manag* 33:75–102. <https://doi.org/10.1007/s11269-018-2089-z>
- Wang H, Pan Y, Chen Y (2017) Comparison of three drought indices and their evolutionary characteristics in the arid region of northwestern China. *Atmos Sci Lett* 18:132–139. <https://doi.org/10.1002/asl.735>
- Wilhite DA (2000) Drought as a natural hazard: Concepts and definitions. *Drought A Glob Assess*
- Xavier AC, King CW, Scanlon BR (2016) Daily gridded meteorological variables in Brazil (1980–2013). *Int J Climatol* 36:2644–2659. <https://doi.org/10.1002/joc.4518>
- Xavier AC, Scanlon BR, King CW, Alves AI (2022) New improved Brazilian daily weather gridded data (1961–2020). *Int J Climatol*. <https://doi.org/10.1002/joc.7731>
- Zalles V, Hansen MC, Potapov PV et al (2019) Near doubling of Brazil's intensive row crop area since 2000. *Proc Natl Acad Sci U S A* 116:428–435. <https://doi.org/10.1073/pnas.1810301115>

**Publisher's Note** Springer Nature remains neutral with regard to jurisdictional claims in published maps and institutional affiliations.

Springer Nature or its licensor (e.g. a society or other partner) holds exclusive rights to this article under a publishing agreement with the author(s) or other rightsholder(s); author self-archiving of the accepted manuscript version of this article is solely governed by the terms of such publishing agreement and applicable law.